Synthesis, Characterization, and Crystal Structure of α-[Ru(azpy)$_2$(NO$_3$)$_2$] (azpy = 2-(Phenylazo)pyridine) and the Products of Its Reactions with Guanine Derivatives

Anna C. G. Hotze,[†] Aldrik H. Velders,[†] Franco Ugozzoli,[‡] Marina Biagini-Cingi,[‡] Anna M. Manotti-Lanfredi,[‡] Jaap G. Haasnoot,[†] and Jan Reedijk*,[†]

Gorlaeus Laboratories, Leiden Institute of Chemistry, Leiden University, P.O. Box 9502, 2300 RA Leiden, The Netherlands, and Dipartimento di Chimica Generale ed Inorganica Chimica, Analitica Chimica, ed Fisica, Università di Parma, and Centro di Studio per la Strutturistica Diffrattometrica del CNR, Parco Area delle Scienze 17/a, 43100 Parma, Italy

Received January 20, 2000

The synthesis and characterization of α-[Ru(azpy)$_2$(NO$_3$)$_2$], **1**, are reported (azpy is 2-(phenylazo)pyridine; α indicates the isomer in which the coordinating pairs ONO$_2$, N(py), and N(azo) are cis, trans, and cis, respectively). The solid-state structure of **1** has been determined by X-ray crystallography. Crystal data: orthorhombic a = 15.423(5) Å, b = 14.034(5) Å, c = 10.970(5) Å, V = 2374(2) Å^3, space group $P2_12_12_1$ (No. 19), Z = 4, D_{calc} = 1.655 g cm^{-3}. The structure refinement converged at R1 = 0.042 and wR2 = 0.118 for 3615 unique reflections and 337 parameters. The octahedral complex shows monodentate coordination of the two nitrate ligands. The Ru−N(azo) bond distances (2.014(4) and 1.960(4) Å), slightly shorter than the Ru−N(py) bonds (2.031(4) and 2.059(4) Å), agree well with the π-back-bonding ability of the azo groups. The binding of the DNA-model bases 9-ethylguanine (9egua) and guanosine (guo) to **1** has been studied and compared with previously obtained results for the binding of model bases to the bis(bipyridyl)ruthenium(II) complex. The ligands 9egua and guo appear to form monofunctional adducts, which have been isolated as α-[Ru(azpy)$_2$(9egua)Cl]PF$_6$, **2**, α-[Ru(azpy)$_2$(9egua)(H$_2$O)](PF$_6$)$_2$, **3**, α-[Ru(azpy)$_2$(guo)(H$_2$O)](PF$_6$)$_2$, **4**, and α-[Ru(azpy)$_2$(guo)Cl]Cl, **5**. The orientations of 9egua and guo in these complexes have been determined in detail with the use of 2D NOESY NMR spectroscopy. In **2** and **5**, H8 is directly pointed toward the coordinated Cl, whereas, in **3** and **4**, H8 is wedged between the pyridine and phenyl rings. The guanine derivatives in the azpy complexes can have more orientations than found for related *cis*-[Ru(bpy)$_2$Cl$_2$] species. This fluxionality is considered to be important in the binding of the α-bis(2-(phenylazo)pyridine)ruthenium(II) complex to DNA. In complex **1**, ruthenium is the chiral center and in the binding to guanosine, two diastereoisomers each of adducts **4** and **5** have been clearly identified by NMR spectroscopy.

Introduction

The binding of the well-known antitumor drug *cis*-[PtCl$_2$(NH$_3$)$_2$] to two neighboring guanines of DNA is generally accepted to be the main interaction responsible for its antitumor activity.[1] At present, a number of antitumor-active ruthenium complexes are known, but no structure−activity relationships (SARs) have been established as yet.[2] It is generally accepted that DNA might also be the target for antitumor-active ruthenium complexes.[2] Therefore it is of interest to study the binding of DNA-model bases to such ruthenium compounds. The compound *cis*-[Ru(bpy)$_2$Cl$_2$] is not antitumor active,[3] even though it has two cis coordinating chloride ligands like cisplatin. Binding of 9-ethylguanine to *cis*-[Ru(bpy)$_2$Cl$_2$] results in the monofunctional compound *cis*-[Ru(bpy)$_2$(9egua)Cl]Cl.[3] Bifunctional coordination to the sterically more hindered six-coordinated octahedral ruthenium complexes is clearly less easy than it is for square-planar complexes, like cisplatin, possibly explaining the lesser activity of the ruthenium complexes.[4] Most interestingly, in contrast to the structurally related bpy complex (Figure 1), α-[Ru(azpy)$_2$Cl$_2$] (in which azpy is 2-(phenylazo)-pyridine) shows a very high cytotoxicity.[5] Unfortunately, α-[Ru(azpy)$_2$Cl$_2$] is poorly soluble in water, whereas, for DNA-binding studies and in vivo testing, reasonable water solubility is required. In this paper, the new water-soluble compound α-[Ru(azpy)$_2$(NO$_3$)$_2$] is presented and its binding to the (DNA-

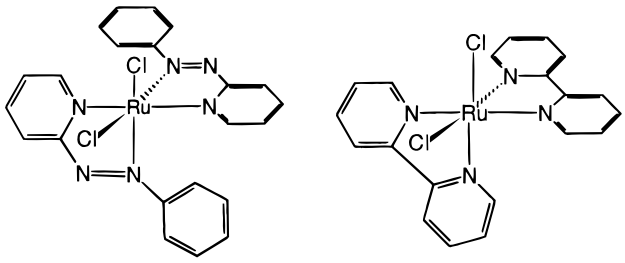

Figure 1. Comparison of the schematic structures of α-[Ru(azpy)$_2$Cl$_2$] and *cis*-[Ru(bpy)$_2$Cl$_2$].

[†] Leiden University.
[‡] Università di Parma and CNR.

(1) Reedijk, J. *Chem. Commun.* **1996**, 801 and references therein.
(2) (a) Keppler, B. K. *Metal Complexes in Cancer Chemotherapy*; VCH Verlagsgesellschaft: Weinheim, Germany, 1993. (b) Clarke, M. J.; Zhu, F.; Frasca, D. R. *Chem. Rev.* **1999**, *99*, 2511.
(3) (a) Nováková, O.; Kašpárková, J.; Vrána, O.; van Vliet, P. M.; Reedijk, J.; Brabec, V. *Biochemistry* **1995**, *34*, 12369. (b) van Vliet, P. M.; Haasnoot, J.; Reedijk, J. *Inorg. Chem.* **1994**, *33*, 1934.
(4) Sherman, S. E.; Gibson, E.; Wang, A. H. J.; Lippard, S. J. *J. Am. Chem. Soc.* **1988**, *110*, 7368.
(5) Velders, A. H.; Kooijman, H.; Spek, A. L.; Haasnoot, J. G.; De Vos, D.; Reedijk, J. *Inorg. Chem.* **2000**, *39*, 2966−2967.

10.1021/ic000066v CCC: $19.00
Published on Web 08/04/2000

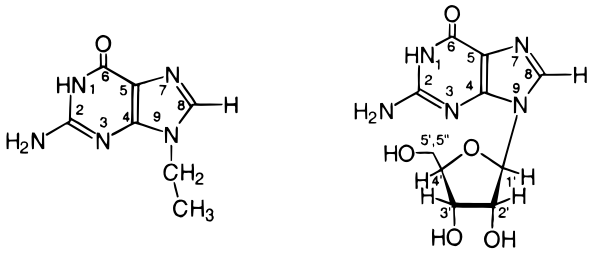

9-ethylguanine (9egua) guanosine (guo)

Figure 2. The DNA model bases 9-ethylguanine and guanosine and their ring-numbering schemes.

model) bases 9-ethylguanine and guanosine (Figure 2) is studied and compared with previously obtained results for the binding of DNA-model bases to *cis*-[Ru(bpy)$_2$Cl$_2$].[3]

Experimental Section

Materials. 9-Ethylguanine (Sigma) and guanosine hydrate (9-D-ribofuranosylguanine) (Aldrich) were obtained commercially and used without purification. 2-(Phenylazo)pyridine,[6] α-[Ru(azpy)$_2$Cl$_2$], and α-[Ru(azpy)$_2$(H$_2$O)$_2$](ClO$_4$)$_2$·H$_2$O were synthesized according to published methods.[7,8] For the synthesis of α-[Ru(azpy)$_2$(9egua)Cl]PF$_6$ and α-[Ru(azpy)$_2$(guo)Cl]Cl, acid aluminum oxide (Alumina Woelm A-Super I) was used.

α-[Ru(azpy)$_2$(NO$_3$)$_2$] (1). Solid AgNO$_3$ (0.60 g, 3.5 mmol) was added to a suspension of α-[Ru(azpy)$_2$Cl$_2$] (0.70 g, 1.3 mmol) in 85 mL of water. The mixture was stirred for 7 days at 40 °C, AgCl was removed by filtration, and 200 mL of ethanol was added to the filtrate. The solution was concentrated to dryness by rotary evaporation, and the residue was dissolved in 400 mL of chloroform. The resulting solution was filtered, and after concentration of the filtrate by rotary evaporation (temperature was kept below 40 °C) and slow addition of diethyl ether, α-[Ru(azpy)$_2$(NO$_3$)$_2$] was isolated as purple crystals, which were suitable for X-ray determination. Yield: 0.61 g (78%). Anal. Calcd for RuC$_{22}$H$_{18}$N$_8$O$_6$: C, 44.7; H, 3.1; N, 18.9. Found: C, 44.6; H, 3.1; N, 18.9. IR (CsI): ν(NO$_3$) 1484, 1274, 989 (broad) cm^{-1}. ^{1}H NMR (chloroform-*d*): δ 9.24 (d, 2H), 8.40 (d, 2H), 8.06 (t, 2H), 7.73 (t, 2H), 7.30 (t, 2H), 7.14 (t, 4H), 6.92 (d, 4H).

α-[Ru(azpy)$_2$(9egua)Cl]PF$_6$ (2). α-[Ru(azpy)$_2$(NO$_3$)$_2$] (0.10 g, 0.17 mmol), dissolved in 28 mL of water, and 9-ethylguanine (0.033 g, 0.19 mmol) were stirred together for 2 days at 40 °C. After filtration, a saturated aqueous solution of NH$_4$PF$_6$ (0.5 g in 1 mL) was added and the precipitate was collected. The product was dissolved in acetone, and the solution was placed on an acid aluminum oxide column. The second fraction (eluent acetone−methanol (10:1)) was isolated and concentrated by rotary evaporation. Diethyl ether was then added, giving pure α-[Ru(azpy)$_2$(9egua)Cl]PF$_6$ as a purple powder. Yield: 0.020 g (14%). Anal. Calcd for RuC$_{29}$H$_{27}$N$_{11}$OClPF$_6$: C, 42.5; H, 3.3; N, 18.6. Found: C, 42.9; H, 3.4; N, 18.8. ESI-MS: *m*/*z* 682, [Ru(azpy)$_2$(9egua)Cl]$^+$.

α-[Ru(azpy)$_2$(9egua)(H$_2$O)](PF$_6$)$_2$ (3). α-[Ru(azpy)$_2$(NO$_3$)$_2$] (0.10 g, 0.17 mmol), dissolved in 28 mL of water, and 9-ethylguanine (0.033 g, 0.19 mmol) were stirred together for 2 days at 40 °C. After filtration, a saturated aqueous solution of NH$_4$PF$_6$ (0.5 g in 1 mL) was added and the precipitate was collected. The purple solid was purified by dissolution in a few milliliters of acetone and addition of diethyl ether. Yield: 0.065 g (41%). Anal. Calcd for RuC$_{29}$H$_{29}$N$_{11}$O$_2$P$_2$F$_{12}$: C, 36.4; H, 3.0; N, 16.1. Found: C, 36.2; H, 2.9; N, 16.1. ESI-MS: *m*/*z* 646.5, [Ru(azpy)$_2$(9egua-H)]$^+$; *m*/*z* 323.8, [Ru(azpy)$_2$(9egua)]$^{2+}$.

α-[Ru(azpy)$_2$(guo)(H$_2$O)](PF$_6$)$_2$ (4). α-[Ru(azpy)$_2$(NO$_3$)$_2$] (0.10 g, 0.17 mmol), dissolved in 29 mL of water, and guanosine (0.053 g, 0.19 mmol) were stirred together for 5 days at 40 °C. After filtration, a saturated aqueous solution of NH$_4$PF$_6$ (0.55 g in 2 mL) was added and the precipitate was collected after the mixture had stood for 16 h at 4 °C. The solid was recrystallized by dissolution in a few milliliters of acetone, removal of any solid residues, and slow addition of diethyl ether. Yield: 0.070 g (39%). ESI-MS: *m*/*z* 750.7, [Ru(azpy)$_2$(guo-H)]$^+$; *m*/*z* 375.9, [Ru(azpy)$_2$(guo)]$^{2+}$.

α-[Ru(azpy)$_2$(guo)Cl]Cl (5). α-[Ru(azpy)$_2$(NO$_3$)$_2$] (0.10 g, 0.17 mmol), dissolved in 29 mL of water, and guanosine (0.054 g, 0.19 mmol) were stirred together for 4 days at 40 °C. After filtration, a saturated aqueous solution of NH$_4$PF$_6$ (0.75 g in 2 mL) was added and the precipitate was collected. The solid was recrystallized by dissolution in acetone followed by filtration and addition of diethyl ether. The solid, dissolved in acetone, was placed on an acid aluminum oxide column. Acetone−methanol (1:10) was used as the eluent. The first two fractions that appeared were discarded. The final fraction, α-[Ru(azpy)$_2$(guo)Cl]Cl, was obtained using 1:20 acetone−methanol as the eluent. Yield: 0.053 g (38%). ESI-MS: *m*/*z* 786, [Ru(azpy)$_2$(guo)Cl]$^+$.

Table 1. Crystallographic Data for α-[Ru(azpy)$_2$(NO$_3$)$_2$] (**1**)

empirical formula	C$_{22}$H$_{18}$N$_8$O$_6$Ru
cryst syst	orthorhombic
space group	$P2_12_12_1$
cell params at 295 K,[a] Å: *a*, *b*, *c*	15.423(5), 14.034(5), 10.970(5)
V, Å^3	2374(2)
Z	4
D_{calcd}, g cm^{-3}	1.655
F(000)	1192
mol wt	591.504
linear abs coeff, cm^{-1}	7.17
radiation	graphite-monochromated Mo Kα (0.710 73 Å)
wR2 (all data)[b]	0.118
a, *b*[b]	0.0795, 0
R1 [$F_o > 4\sigma(F_o)$][b]	0.042
no. of obsd reflns	3615
goodness-of-fit on F^2 (all data)[b]	0.89
max shift/σ	0.07
peak, hole in final diff map, e Å^{-3}	+2.08, −1.1
extinction coeff	0.006 37

[a] Unit cell parameters were obtained by least-squares analysis of the setting angles of 28 reflections found in a random search on the reciprocal space in the range $12 \le \theta \le 18°$. [b] $R_1 = \sum||F_o| - |F_c||/\sum|F_o|$; wR2 = $[\sum w(F_o^2 - F_c^2)^2/\sum wF_o^4]^{1/2}$; goodness-of-fit = $[\sum w(F_o^2 - F_c^2)^2/(n - p)]^{1/2}$, where *n* is the number of reflections and *p* the number of parameters.

Methods and Instrumentation. NMR experiments were performed at 300.13 MHz on a Bruker 300 DPX spectrometer. Spectra were recorded in D$_2$O, calibrated on the H$_2$O peak, and acetone-*d*$_6$, calibrated on the CD$_2$HCOCD$_3$ peak (δ 2.06). All spectra were obtained at 25 °C unless otherwise noted. 2D ^{1}H−^{1}H NOESY experiments were performed with a mixing time of 1 s, eight scans per t_1 increment, and a relaxation delay of 1 s. IR spectra were recorded on a Perkin-Elmer Paragon 1000 FT-IR spectrometer for samples in CsI pellets. Elemental analyses (C, H, and N) were carried out by the Chemical Services Unit of University College Dublin and by Gorlaeus Laboratories of Leiden University. Mass spectra were obtained by Gorlaeus Laboratories on a Finnigan MAT 900 instrument equipped with an electrospray interface (ESI). Potentiometric pH titrations were carried out with a Metrohm 691 pH meter equipped with a Schott Geräte T80/10 and a combination pH electrode (Russell, CER7). The direct pH-meter readings were used to calculated the pK_a values.

Single-Crystal X-ray Analysis of 1. Compound **1** was crystallized from a mixture of chloroform and diethyl ether. A purple single-crystal of approximate dimensions 0.2 × 0.2 × 0.3 mm^3 suitable for X-ray analysis was isolated and mounted on a Siemens AED diffractometer equipped with graphite-monochromated Mo Kα radiation (λ = 0.710 73 Å). The single-crystal X-ray diffraction experiments were carried out at 295 K, and the unit cell parameters, reported in Table 1, were obtained by a least-squares fit of 28 $I(\theta\kappa\phi)_{hkl}$ reflections in the range $12 \le \theta \le 18°$. The systematic absences *h*00, *h* odd, 0*k*0, *k* odd, and 00*l*, *l* odd, led to the $P2_12_12_1$ (No. 19) space group. A total of 7539 $\pm h,+k,+l$ ($-21 \le h \le 21$, $0 \le k \le 19$, $0 \le l \le 15$) reflections, of which 6144 were unique (R_{int} = 0.016), were measured by the $\omega/2\theta$

(6) Krause, R. A.; Krause, K. *Inorg. Chem.* **1980**, *19*, 2600.
(7) Bao, T.; Krause, K.; Krause, R. A. *Inorg. Chem.* **1988**, *27*, 759.
(8) Goswami, S.; Chakravarty, A. R.; Chakravorty, A. *Inorg. Chem.* **1983**, *22*, 602.

scan technique in the range $3 \leq \theta \leq 30°$, and the intensities were calculated from the analysis of the diffraction profiles according to the Lehmann and Larsen method.[9] During the systematic data collection, one standard reflection monitored every 100 reflections indicated no significant fluctuations. The collected intensities were corrected for Lorentz and polarization effects but not for absorption.

The structure was solved by direct methods using SIR92;[10] the *E* map revealed the positions of the metal atom and the atoms of the coordination sphere. The remaining atoms were located by successive cycles of Fourier ΔF maps. The structure was refined by full-matrix least-squares calculations on F^2 with SHELX-96[11] using anisotropic atomic displacements for all non-hydrogen atoms. All hydrogen atoms were added to the corresponding C atoms in the "riding" model, with the geometrical constraint C−H = 0.96 Å), and refined with isotropic atomic displacements. The final cycle of refinement included 6144 reflections and 337 parameters (zero restraints) and converged to R1 = 0.042 and wR2 = 0.118 with a goodness of fit $S = 0.89$. No unusual trends were found in F_o^2 versus F_c^2 as a function of $(\sin\theta)/\lambda$, in the Miller indices, and in F_o^2. All geometrical calculations were obtained by PARST[12] on a DEC Alpha 250 workstation at the Centro di Studio per la Strutturistica Diffrattometrica del CNR. The final CIF file for the strucure determination of complex **1** has been deposited at the CCDC under Deposition No. 136743.

Results and Discussion

General Information. It is known that α-[Ru(azpy)$_2$Cl$_2$] can isomerize to the β isomer, but the exact conditions for this to occur are not yet fully understood.[7,13] In fact, in an attempt to prepare **3** and **4** under refluxing conditions, isomerization to the β isomers was observed. Our experiments at various temperatures indicate that isomerization from the α isomer to the β isomer in aqueous solution does not occur at or below 40 °C. For this reason, the synthesis of α-[Ru(azpy)$_2$(NO$_3$)$_2$], **1**, and the reactions of **1** with DNA-model bases were carried out at 40 °C.

Prior to the synthesis of **1**, the coordination of the nitrate ligand in this compound was uncertain. The NO_3^- ion can be noncoordinating, or it can coordinate in a didentate (NO_3-*O*,*O*′) or monodentate (NO_3-*O*) fashion.[14] So, in theory, one could expect one or more of the following complexes: α-[Ru(azpy)$_2$(H$_2$O)$_2$](NO$_3$)$_2$, α-[Ru(azpy)$_2$(H$_2$O)(NO_3-*O*)]NO$_3$, α-[Ru(azpy)$_2$(NO$_3$-*O*)$_2$], and α-[Ru(azpy)$_2$(NO_3-*O*,*O*′)]NO$_3$. For this reason, recrystallizations from ethanol and chloroform were performed to reduce the number of possibilities. This procedure resulted in the isolation of only the neutral complex in which the two nitrate ions are coordinated as monodentate ligands, α-[Ru(azpy)$_2$(NO$_3$-*O*)$_2$]. The N−O stretching vibrations in the IR spectrum were found at 1484, 1274, and 989 cm^{-1}. From these values which are in accordance with literature values,[14] it is not possible to distinguish between mono- and didentate coordinations of the NO_3^- ion. The X-ray data, however, clearly indicate monodentate coordination of the NO_3^- ions (vide infra).

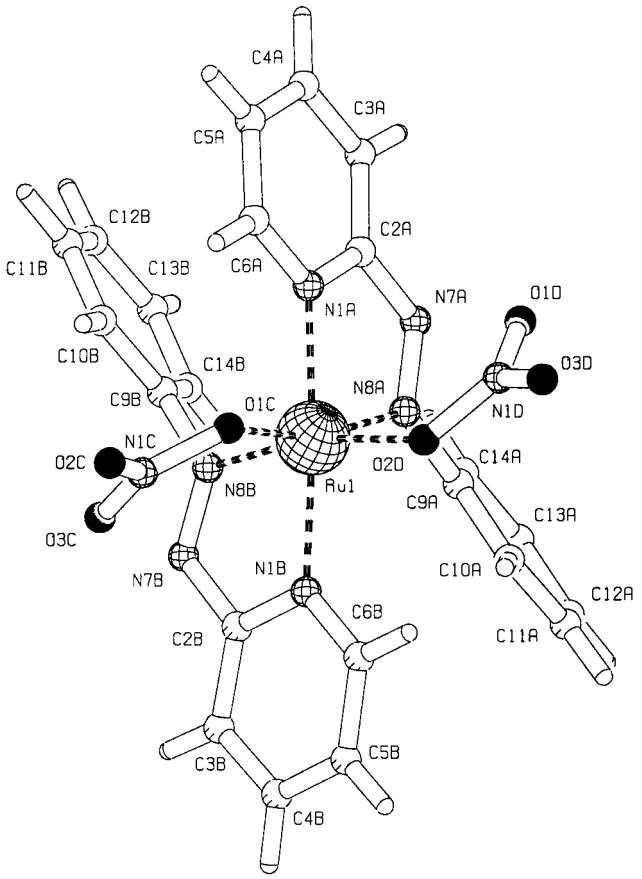

Figure 3. Molecular structure and atomic numbering of α-[Ru(azpy)$_2$(NO$_3$)$_2$], **1**.

In the reactions of α-[Ru(azpy)$_2$(NO$_3$)$_2$] with DNA-model bases (L′ = 9egua and guo) with varying reagent ratios and reaction times, no bifunctional adducts of the formula [Ru(azpy)$_2$(L′)$_2$] were obtained. When α-[Ru(azpy)$_2$(9egua)(H$_2$O)](PF$_6$)$_2$ and α-[Ru(azpy)$_2$(guo)(H$_2$O)](PF$_6$)$_2$ were placed on an acid alumina column, the coordinated H$_2$O was substituted by Cl$^-$ on ruthenium. Also the PF_6^- counterion could be exchanged with Cl$^-$, which occurred for α-[Ru(azpy)$_2$(guo)(H$_2$O)](PF$_6$)$_2$. The exact conditions for the exchange of PF_6^- with Cl$^-$, which probably depend on the amount of solid and size of the column, are not clear.

Characterization of α-[Ru(azpy)$_2$(NO$_3$)$_2$]. A projection of the X-ray structure of α-[Ru(azpy)$_2$(NO$_3$)$_2$], **1**, is shown in Figure 3. Table 1 lists the crystallographic data for α-[Ru(azpy)$_2$(NO$_3$)$_2$], and relevant bond distances and angles are given in Table 2. If the coordinating pairs of NO_3^-, N(py), and N(azo) are considered in that order, the configuration of **1** is cis,trans,cis (ctc). The crystal structure clearly shows monodentate coordination of the nitrate ligands (the Ru−O distances are 2.091(4) and 2.086(5) Å). The Ru−N(azo) distances (2.014(4) and 1.960(4) Å) are slightly shorter than the Ru−N(py) distances (2.031(4) and 2.059(4) Å). In the crystal structures of

(9) Lehmann, M. S.; Larsen, F. K. *Acta Crystallogr., Sect. A* **1974**, *A30*, 580.
(10) Altomare, A.; Burla, M. C.; Camalli, M.; Cascarano, G.; Giacovazzo, C.; Guagliardi, A.; Polidori, G. SIR92. *J. Appl. Crystallogr.* **1994**, *27*, 435.
(11) Sheldrick, G. M. *SHELXL-96*: *Program for Crystal Structure Refinement*; University of Göttingen: Göttingen, Germany, 1996.
(12) Nardelli, M. PARST. *Comput. Chem.* **1983**, *7*, 95.
(13) Krause, R. A.; Krause, K. *Inorg. Chem.* **1982**, *21*, 1714.
(14) (a) Nakamoto, K. *Infrared and Raman Spectra of Inorganic and Coordination Compounds*; John Wiley & Sons: New York, 1986, (b) Steed, J. W.; Tocher, D. *Polyhedron* **1994**, *13*, 167.
(15) Seal, A.; Ray, S. *Acta Crystallogr., Sect. C* **1984**, *C40*, 929.
(16) Korn, S.; Sheldrick, W. S. *J. Chem. Soc., Dalton Trans.* **1997**, 2191.
(17) van Vliet, P. M.; Toekimin, S. M. S.; Haasnoot, J. G.; Reedijk, J.; Nováková, O.; Vrána, O.; Brabec, V. *Inorg. Chim. Acta* **1995**, *231*, 57.
(18) Iwamoto, M.; Alessio, E.; Marzilli, L. G. *Inorg. Chem.* **1996**, *35*, 2384.
(19) Marzilli, L. G.; Marzilli, P. A.; Alessio, E. *Pure Appl. Chem.* **1998**, *70*, 961.
(20) Chatterjee, D.; Ward, M. S.; Shepherd, R. E. *Inorg. Chim. Acta* **1999**, *285*, 170.
(21) Song, B.; Zhao, J.; Griesser, R.; Meiser, C.; Sigel, H.; Lippert, B. *Chem.—Eur. J.* **1999**, *5*, 2374.
(22) Cramer, R. E.; Dahlstrom, P. L. *J. Am Chem. Soc.* **1979**, *101*, 3679.
(23) Grover, N.; Gupta, N.; Thorp, H. H. *J. Am. Chem. Soc.* **1992**, *114*, 3390.
(24) Hotze, A. C. G. To be published.
(25) Velders, A. H. To be published.

Table 2. Selected Bond Distances (Å) and Angles (deg) of Complex **1**

Ru−N(1A)	2.031(4)	Ru−N(1B)	2.059(4)
Ru−N(8A)	2.014(4)	Ru−O(1C)	2.091(4)
Ru−N(8B)	1.960(4)	Ru−O(2D)	2.087(4)
N(8A)−N(7A)	1.282(5)	N(8B)−N(7B)	1.270(5)
N(8A)−C(9A)	1.432(6)	N(8B)−C(9B)	1.437(6)
N(7A)−C(2A)	1.391(6)	N(7B)−C(2B)	1.400(6)
N(1C)−O(1C)	1.311(6)	N(1D)−O(1D)	1.215(6)
N(1C)−O(2C)	1.218(6)	N(1D)−O(2D)	1.294(6)
N(1C)−O(3C)	1.209(7)	N(1D)−O(3D)	1.221(6)
N(1A)−Ru−O(2D)	96.2(1)	N(8A)−Ru−O(2D)	96.7(1)
O(2D)−Ru−N(1B)	91.3(2)	N(8A)−Ru−N(1B)	100.9(2)
N(1B)−Ru−N(8B)	76.3(2)	O(1C)−Ru−O(2D)	77.9(1)
N(8B)−Ru−N(1A)	96.3(2)	O(1C)−Ru−N(1A)	90.3(1)
N(8A)−Ru−N(8B)	87.2(2)	O(1C)−Ru−N(8B)	100.9(2)
N(8A)−Ru−N(1A)	76.7(1)	O(1C)−Ru−N(1B)	92.9(2)
N(8A)−Ru−O(1C)	165.4(1)	N(8B)−Ru−O(2D)	167.5(2)
N(7A)−N(8A)−Ru	119.6(3)	N(7B)−N(8B)−Ru	122.7(3)
C(9A)−N(8A)−Ru	127.5(3)	C(9B)−N(8B)−Ru	123.0(3)
N(7A)−N(8A)−C(9A)	112.7(4)	N(7B)−N(8B)−C(9B)	113.7(4)
C(2A)−N(1A)−Ru	113.3(3)	C(2B)−N(1B)−Ru	112.3(3)
C(6A)−N(1A)−Ru	128.5(3)	C(6B)−N(1B)−Ru	129.3(3)

α-[Ru(azpy)$_2$Cl$_2$] and *β*-[Ru(azpy)$_2$Cl$_2$], the relatively short Ru−N(azo) distances have been explained by the occurrence of *π*-back-bonding.[15] The N═N distances in **1** (1.270(5) and 1.282(5) Å) are similar to the N═N distances in α-[Ru(azpy)$_2$Cl$_2$] (1.279(7) and 1.283(6) Å). The bite angles N(8A)−Ru−N(1A) and N(8B)−Ru−N(1B) [76.7(1) and 76.23(2)°] reveal a considerable distortion in the octahedron around Ru and are similar to the ones found for α-[Ru(azpy)$_2$Cl$_2$]. The angle O(1C)−Ru−O(2D) is small too, 77.9(1)°, and contributes to the distortion of the octahedron. The octahedral distortion observed in complex **1** is more pronounced than that observed in the α-[Ru(azpy)$_2$Cl$_2$] complex, as shown by the sums of the bond angles in the equatorial planes (362° in **1** vs 360° in α-[Ru(azpy)$_2$Cl$_2$]); however, it is noteworthy that this distortion could be induced by the network of hydrogen bonds (see Figure S5 and Table SI in the Supporting Information), which involve the two nitrato anions and the C−H groups from pyridine moieties of neighboring complexes. No stacking interactions have been observed in the lattice.

The ^{1}H NMR spectrum of **1** in acetone-d_6 (Table 3) shows only one set of azpy peaks, indicating two equivalent azpy ligands, so the complex must be symmetric due to its C_2 axis. The assignment is made with the use of 2D COSY NMR spectroscopy, and H6 and H3 are assigned on the basis of the ^3J coupling constants, which are larger for H3. In the ^{1}H NMR spectrum, only one resonance each is observed for the ortho and meta hydrogens as free rotation of the phenyl ring about the C−N axis on the NMR time scale occurs. In a 2D NOESY spectrum, the α configuration is confirmed by a strong NOE cross-peak between the H6 and ortho-hydrogen signals, which is in accordance with the determined distance in the crystal structure (2.4 Å). In comparison with those of α-[Ru(azpy)$_2$(H$_2$O)$_2$](ClO$_4$)$_2$·H$_2$O, NMR measurements show that, in acetone, complex **1** remains intact with NO_3^- coordinated but, in water, **1** solvolyzes to form α-[Ru(azpy)$_2$(H$_2$O)$_2$](NO$_3$)$_2$.

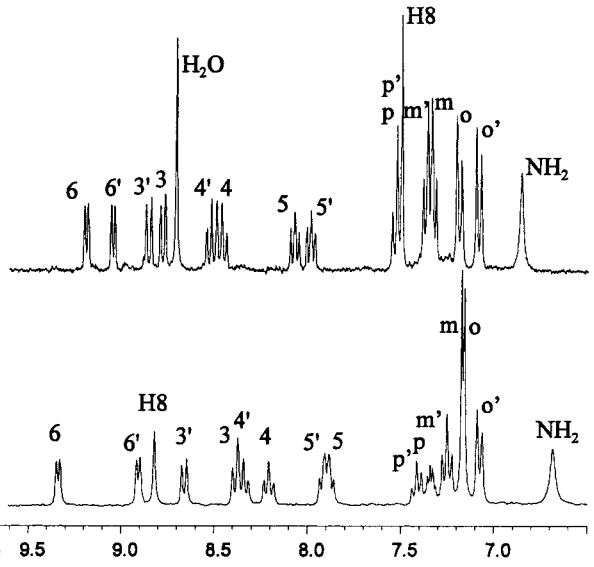

Figure 4. Aromatic regions of the ^{1}H NMR spectra of α-[Ru(azpy)$_2$(9egua)(H$_2$O)](PF$_6$)$_2$ (upper) and α-[Ru(azpy)$_2$(9egua)Cl]PF$_6$ (lower) in acetone-d_6 at 25 °C.

NMR Structural Characterization of the Products of the Reaction of 1 with Model Bases. α-[Ru(azpy)$_2$(9egua)Cl]PF$_6$. The 1:1 reaction of 9egua with α-[Ru(azpy)$_2$(NO$_3$)$_2$] results in the formation of α-[Ru(azpy)$_2$(9egua)Cl]PF$_6$, as concluded from the ^{1}H NMR spectrum (Figure 4, Table 3). The first indication of the 1:1 adduct of **1** with 9egua stems from the fact that the two azpy ligands are no longer identical, as deduced from two sets of signals in the NMR spectrum. Although, in theory, an asymmetric bisadduct would also result in two sets of azpy signals, the integration of the ethyl signals and the H8 signal to the azpy signals confirms the monofunctional coordination of 9egua. The 9egua ligand coordinates to Ru through its N7 atom, as confirmed by a pH titration (vide infra) showing that N7 protonation is absent.[3] The assignment of the signals was made from 2D NOESY and COSY NMR data. The interligand NOE cross-peaks between the H6 and ortho signals, H6−o′ and H6′−o, confirm the configuration of the α-isomer. Important signals of coordinated 9egua are the broad NH signal at 10.5 ppm, the H8 signal at 8.82 ppm, and the NH$_2$ signal at 6.70 ppm. The position of the H8 signal of 9egua is determined by its intraligand NOE cross-peaks with the signals of the ethyl group of 9egua. H8 of 9egua has an NOE cross-peak with H6 of one azpy ligand and a cross-peak with H6′ of the other azpy ligand (Figure 5). This indicates the orientation of 9egua with its H8 pointed toward the coordinated Cl atom.

α-[Ru(azpy)$_2$(9egua)(H$_2$O)](PF$_6$)$_2$. The ^{1}H NMR spectrum of α-[Ru(azpy)$_2$(9egua)(H$_2$O)](PF$_6$)$_2$ (Figure 4, Table 3) in acetone-d_6 shows azpy signals that are all different from those of α-[Ru(azpy)$_2$(9egua)Cl]PF$_6$ in acetone-d_6. Again signals in

Table 3. Proton Chemical Shift Values (ppm) for α-[Ru(azpy)$_2$(NO$_3$)$_2$] (**1**), α-[Ru(azpy)$_2$(9egua)Cl]PF$_6$ (**2**), and α-[Ru(azpy)$_2$(9egua)(H$_2$O)](PF$_6$)$_2$ (**3**) in D$_2$O (a) and Acetone-d_6 (b)

	H6/6′	H3/H3′	H4/H4′	H5/H5′	p/p′	m/m′	o/o′	H8
1 (a)[a]	8.73	8.67	8.31	7.84	7.38	7.20	6.81	
1 (b)	9.18	8.54	8.32	8.04	7.41	7.29	7.05	
2 (a), pH 3.5	9.03/8.54	8.20/8.46	8.05/8.20	7.70/7.70	7.27/7.29	7.14/7.10	6.90/6.90	8.58
2 (b)	9.35/8.90	8.39/8.66	8.21/8.34	7.88/7.91	7.34/7.40	7.25/7.25	7.20/7.06	8.82
3 (a),[b] pH <6	8.90/8.58	8.62/8.73	8.28/8.37	7.87/7.80	7.46/7.46	7.27/7/27	6.90/7.00	7.1
3 (b)	9.19/9.04	8.78/8.86	8.47/8.52	8.08/8.00	7.52/7.52	7.36/7.34	7.20/7.10	7.48

[a] α-[Ru(azpy)$_2$(D$_2$O)$_2$]$^{2+}$. [b] α-[Ru(azpy)$_2$(9egua)(D$_2$O)]$^{2+}$.

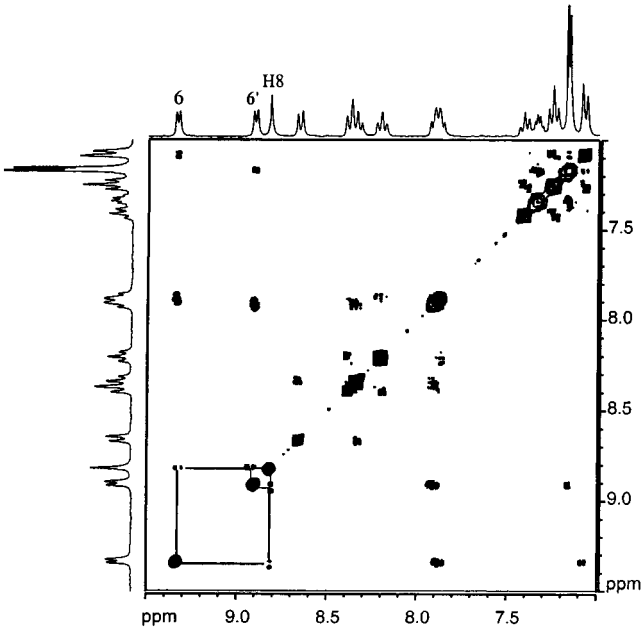

Figure 5. 2D ^{1}H−^{1}H NOESY spectrum and some assignments (proton numbering as in Figure 7) of the aromatic region of α-[Ru(azpy)$_2$(9-egua)Cl]PF$_6$ in acetone-d_6 at 25 °C. The H8−H6 and H8−H6′ NOEs are indicated by solid lines.

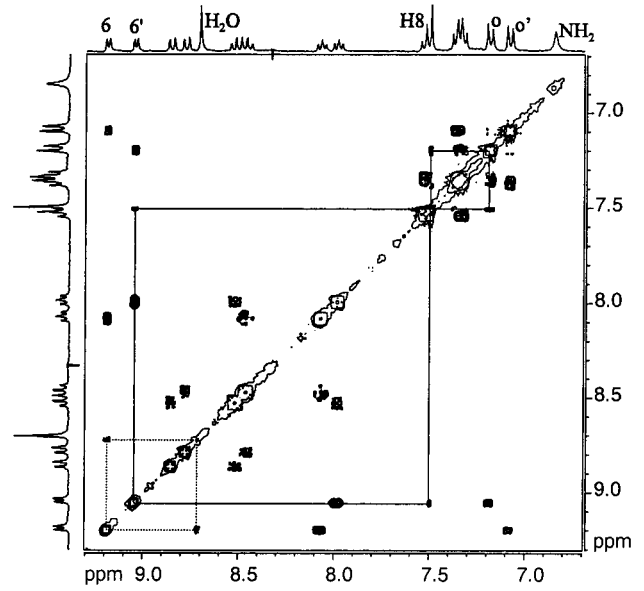

Figure 6. 2D ^{1}H−^{1}H NOESY spectrum and some assignments (proton numbering as in Figure 7) of the aromatic region of α-[Ru(azpy)$_2$(9-egua)(H$_2$O)](PF$_6$)$_2$ in acetone-d_6 at 25 °C. The H8−Ho and H8−H6′ NOEs are indicated by solid lines; the H6−H$_2$O NOE is indicated by dotted lines.

the aromatic region of the coordinated 9egua are the broad NH resonance at 11.2 ppm, the NH$_2$ signal at 6.86 ppm, and the H8 signal at 7.48 ppm. Striking differences from the ^{1}H NMR spectrum of α-[Ru(azpy)$_2$(9egua)Cl]PF$_6$ in acetone-d_6 are the position of the H8 peak at relatively high field and the presence of the coordinated H$_2$O peak at 8.70 ppm. The coordinated water gives a strong NOE cross-peak with H6. NMR measurements of **3** in D$_2$O at room temperature show a broad H8 peak, which sharpens at higher temperatures, indicating some fluxionality of the 9egua model base.

The 2D NOESY spectrum of α-[Ru(azpy)$_2$(9egua)(H$_2$O)](PF$_6$)$_2$ in acetone-d_6 (Figure 6) shows NOE cross-peaks between the H8 and H6′ signals and between the H8 and ortho-hydrogen

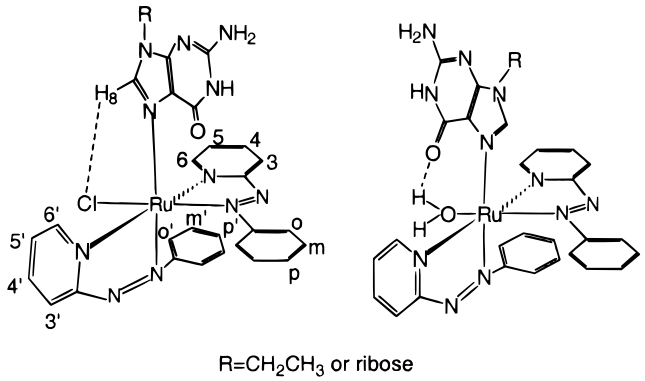

Figure 7. Orientations of 9egua and guo (L) in α-[Ru(azpy)$_2$LCl]$^+$ and α-[Ru(azpy)$_2$L(H$_2$O)]$^{2+}$ (with the numbering used for the NMR assignments).

signals. This indicates that H8 of the coordinated 9egua is wedged between the pyridine ring and phenyl ring. In this position, a hydrogen bond between the coordinated water and the keto group of 9egua is likely to stabilize this conformation. Such intramolecular hydrogen-bond formation of the keto group of coordinated 9egua with coordinated H$_2$O has been shown in the crystal structure[16] of [Ru(η^6-C$_6$H$_6$)(9egua)$_2$(H$_2$O)](CF$_3$SO$_3$)$_2$ and proposed[17] in the complex *trans*-[Ru(terpy)$_2$(9-egua)$_2$(H$_2$O)]-(PF$_6$)$_2$.

Orientation of 9egua in the Complexes. As discussed above, the NOESY NMR data of the compounds α-[Ru(azpy)$_2$-(9egua)Cl]PF$_6$, **2**, and α-[Ru(azpy)$_2$(9egua)(H$_2$O)](PF$_6$)$_2$, **3**, indicate that 9egua can have more than one orientation (Figure 7). In **2**, H8 points toward the Cl atom, and in **3**, H8 is wedged between the pyridine and phenyl rings and the keto group is above the H$_2$O ligand. The downfield shift of the H8 signal of **2** relative to that of **3** is a further indication of this different 9egua orientation, and the downfield shift is likely caused by the Cl atom.[18] The downfield shift of the H8 signal of **2** in comparison to that of **3** might be caused only by the influence of the Cl ligand,[18] but the NOE signals indicate different orientations of 9egua in **2** and **3**. The orientation of 9egua in **2** could be influenced by the electrostatic attraction between the N$_2$C$^{\delta+}$ proton and the negative Cl ligand, which was suggested recently for complexes such as *cis*,*cis*,*cis*-[RuCl$_2$(Me$_2$SO)$_2$L$_2$] with L = lopsided N-heterocyclic ligands.[19] When the water ligand is coordinated in **3**, this attraction is no longer present and the possibility of hydrogen bonding might favor the orientation of the keto group above the H$_2$O ligand. These scenarios do not permit to conclude which orientation of 9egua is sterically more favorable.

Hydrolysis of α-[Ru(azpy)$_2$(9egua)Cl]$^+$. α-[Ru(azpy)$_2$(9egua)-(H$_2$O)]$^{2+}$ is formed in situ by addition of AgNO$_3$ to **2** in D$_2$O as the Cl ligand of α-[Ru(azpy)$_2$(9egua)Cl]$^+$ is substituted. The NH and H$_2$O signals are not visible in D$_2$O, but the H8 signal shows a shift from 8.58 ppm in α-[Ru(azpy)$_2$(9egua)Cl]$^+$ (Table 3) to a broad signal at 7.10 ppm in α-[Ru(azpy)$_2$(9egua)(D$_2$O)]$^{2+}$ (Table 3). This shift of the H8 signals is in agreement with the shift of the H8 signals of **2** and **3** in acetone-d_6. The chloride in α-[Ru(azpy)$_2$(9egua)Cl]$^+$ is replaced faster than that in *cis*-[Ru(bpy)$_2$(9egua)Cl]$^+$ (in *cis*-[Ru(bpy)$_2$(9egua)Cl]$^+$ the chloride remains coordinated during 24 h at 37 °C, whereas α-[Ru(azpy)$_2$-(9egua)(D$_2$O)]$^{2+}$ is already 50% formed from α-[Ru(azpy)$_2$-(9egua)Cl]$^+$ after about 35 min at 37 °C). The fact that the azpy ligand is a better trans-labilizing ligand than bpy[7] might be related to the faster hydrolysis rate of **2**.

(De)protonation of α-[Ru(azpy)$_2$(9egua)(Cl/H$_2$O)](PF$_6$)$_{1/2}$. The 9egua ligand in α-[Ru(azpy)$_2$(9egua)Cl]PF$_6$, **2**, coordinates

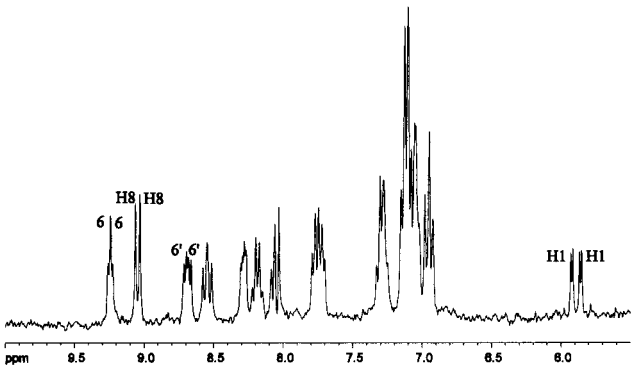

Figure 8. Aromatic region of the ^{1}H NMR spectrum of α-[Ru(azpy)$_2$(guo)Cl]Cl in methanol-d_4 at 25 °C.

Scheme 1 Deprotonation Scheme for α-[Ru(azpy)$_2$(9egua)(H$_2$O)](PF$_6$)$_2$

α-[Ru(azpy)$_2$(9egua)(H$_2$O)]$^{2+}$

⇅ pH~4

α-[Ru(azpy)$_2$(9egua)(OH)]$^+$

⇅ pH~7

α-[Ru(azpy)$_2$(9egua-H)(OH)]

to ruthenium through its N7 atom, as confirmed by a pH titration in the range from pH 1 to pH 12, showing the absence of N7 protonation.[3] The titration curve shows the (de)protonation of N1 of 9egua in **2** at ca. pH = 8.5. The (de)protonation of α-[Ru(azpy)$_2$(9egua)(H$_2$O)](PF$_6$)$_2$ (Scheme 1) was studied by NMR spectroscopy in D$_2$O. In D$_2$O at pH < 5, both the coordinated D$_2$O and 9egua are protonated and lowering the pH to 2 results in no significant changes in the spectrum. With increasing pH (pH >5), signals in the NMR spectra show a shift and new signals appear. Both the N1 of 9egua and coordinated water deprotonate, and the color of the solution changes from purple to blue. Such a color change was also observed[20] for N1 deprotonation of 5′-GMP in [Ru^{III}(edta)(5′-GMP)], and a pK_a value for N1 of 7.2 was given. In the present case, the color change of α-[Ru(azpy)$_2$(9egua)(H$_2$O)](PF$_6$)$_2$ might also occur due to deprotonation of the coordinated H$_2$O. A potentiometric titration of α-[Ru(azpy)$_2$(9egua)(H$_2$O)](PF$_6$)$_2$ gives a pK_a value for the coordinated water ligand of ca. 4, which is comparable to the pK_a values of coordinated water in related platinum complexes.[21] The pK_a for N1 of 9egua in α-[Ru(azpy)$_2$(9egua)(H$_2$O)](PF$_6$)$_2$ is ca. 7, similar to the value[20] of 7.2 for N1 of 5′-GMP in [Ru^{III}(edta)(5′-GMP)] mentioned above.

Reaction of α-[Ru(azpy)$_2$(NO$_3$)$_2$] with Guanosine. The reaction of α-[Ru(azpy)$_2$(NO$_3$)$_2$] with guanosine followed by elution on an alumina column, acidified with HCl, yielded the compound α-[Ru(azpy)$_2$(guo)Cl]Cl, **5**. The presence of two diastereoisomers of **5** is clearly seen in its ^{1}H NMR spectrum (Figure 8). α-[Ru(azpy)$_2$(NO$_3$)$_2$] is a racemic mixture, containing equal amounts of Δ and Λ enantiomers, and with the use of guanosine (D-guanosine), two diastereoisomers of adduct **5** are to be expected.[22] Indeed, a double set of signals is observed in the NMR spectrum. Best seen are the two sugar H1 signals and four H6 signals (two for each diastereoisomer) (Figure 8). The positions of the H8 signals of guo in both diastereoisomers at 9.06 and 9.03 ppm are confirmed by the intraligand NOE cross-peak between the sugar H1 signal and the H8 signal. The H8 signal has interligand NOE cross-peaks with the H6 signal of one azpy ligand and the H6′ signal of the other azpy ligand. These NOE cross-peaks and the fact that the H8 signals of both diastereoisomers appear at relatively low field are the same results as found for the complex α-[Ru(azpy)$_2$(9egua)Cl]PF$_6$ and indicate that H8 points toward the Cl ligand, as depicted in Figure 7.

^{1}H NMR spectrum of α-[Ru(azpy)$_2$(guo)(H$_2$O)](PF$_6$)$_2$, **4**, in acetone-d_6 indicates again the presence of two diastereoisomers, the two H8 signals appearing at 7.79 and 7.62 ppm, i.e., at relatively high field. The 2D NOESY NMR spectrum of **4** in acetone-d_6 shows NOE cross-peaks for H8−o and H8−6′, indicating H8 of the coordinated guo to be wedged between the pyridine and phenyl rings. The NMR data of **4** and **5** show that guo can have more than one orientation, as found for 9egua in **2** and **3**. Ruthenium complexes are known to interact with DNA stereoselectively,[23] but with the use of guanosine, no enantioselective binding has been found. To investigate the possible stereoselective interaction of α-[Ru(azpy)$_2$] with DNA in vivo, the binding of **1** with oligonucleotides is currently being investigated.

Summary

Because of the strong differences in biological activity between the structurally similar complexes *cis*-[Ru(bpy)$_2$Cl$_2$] and α-[Ru(azpy)$_2$Cl$_2$], it is important to compare the bindings of DNA-model bases to both complexes in search for a structure−activity relationship. In this paper α-[Ru(azpy)$_2$(NO$_3$)$_2$], which is the water-soluble analogue of the cytotoxic complex α-[Ru(azpy)$_2$Cl$_2$], and its binding to guanine derivatives are described. The DNA-model base 9egua coordinates to both *cis*-[Ru(bpy)$_2$] and α-[Ru(azpy)$_2$] moieties monofunctionally via the N7 atom. This similarity in 9equa coordination does not explain the difference in cytotoxicity of the two complexes, and for this reason, studies investigating the binding of other DNA-model bases, such as adenine derivatives, and factors influencing coordination and orientation of DNA-model bases are being conducted.[24] The crystal structure of *cis*-[Ru(bpy)$_2$(9egua)Cl]PF$_6$ shows[3] that the keto group of egua is "stacked" between two pyridyl rings of the bpy ligands. From NMR data, it has been concluded that there are no rotamers of *cis*-[Ru(bpy)$_2$(9egua)-Cl]PF$_6$, in contrast to the case of the azpy analogue mentioned above. In fact, the larger but more flexible azpy ligand appears to allow more orientations for the guanine derivatives. The α-[Ru(azpy)$_2$] moiety being more flexible in its coordination to heterocycles than the *cis*-[Ru(bpy)$_2$] moiety is in agreement with studies on the rotational behaviors of the smaller model base 1-MeBim in α-[Ru(azpy)$_2$(1-MeBim)$_2$](PF$_6$)$_2$ and *cis*-[Ru(bpy)$_2$(1-MeBim)$_2$](PF$_6$)$_2$.[25] Although, in the case of *cis*-[Ru(bpy)$_2$Cl$_2$] reacting with 9egua, only the monofunctional adduct *cis*-[Ru(bpy)$_2$(9egua)Cl]Cl could be isolated,[3] bifunctional binding to two nucleobases in DNA cannot be excluded.[26] The binding of different N-heterocycles to *cis*-[Ru(bpy)$_2$Cl$_2$] shows[27,28] that this complex is a borderline case, in which the type of coordination of the heterocycles depends on relatively small steric differences in the ligands. For this reason, the possibility of bifunctional coordination of the α-[Ru(azpy)$_2$] moiety to DNA in vivo should not be excluded and therefore the reactions of α-[Ru(azpy)$_2$(NO$_3$)$_2$] with oligonucleotides are of interest. Studies of such reactions are currently in progress.

(26) Grover, N.; Welch, T. W.; Fairly, A. T.; Cory, M.; Thorp, H. H. *Inorg. Chem.* **1994**, *33*, 3544.
(27) Velders, A. H.; Hotze, A. C. G.; Haasnoot, J. G.; Reedijk, J. *Inorg. Chem*. **1999**, *38*, 2762.
(28) Velders, A. H.; Hotze, A. C. G.; Haasnoot, J. G.; Reedijk, J. *Inorg. Chem.*, in press.

Acknowledgment. We thank Johnson Matthey Chemicals for a generous loan of $RuCl_3 \cdot 3H_2O$. This research was sponsored by the Council for Chemical Sciences of The Netherlands Organization for Scientific Research. Additional support from COST Action D8 (Chemistry of Metals in Medicine), the Italian MURST, and the CNR is also gratefully acknowledged.

Supporting Information Available: An ^{1}H NMR spectrum of **1** in acetone-d_6, a pH titration curve for **2**, 2D NOESY spectra of **4** and **5**, a figure showing the crystal lattice of **1** with its network of hydrogen bonds, a table of relevant hydrogen bond data for the crystal lattice of **1**, and an X-ray crystallographic file, in CIF format, for the crystal structure determination of **1**. This material is available free of charge via the Internet at http://pubs.acs.org.

IC000066V